BJP BRITISH JOURNAL OF PHARMACOLOGY

BPS BRITISH PHARMACOLOGICAL SOCIETY

British Journal of Pharmacology (2010), 160, 1699–1713

0007-1188/10
www.brjpharmacol.org

RESEARCH PAPER

# A novel, orally active $LPA_1$ receptor antagonist inhibits lung fibrosis in the mouse bleomycin model

JS Swaney, C Chapman, LD Correa, KJ Stebbins, RA Bundey, PC Prodanovich, P Fagan, CS Baccei, AM Santini, JH Hutchinson, TJ Seiders, TA Parr, P Prasit, JF Evans and DS Lorrain

*Amira Pharmaceuticals, San Diego, CA, USA*

**Background and purpose:** The aim of this study was to assess the potential of an antagonist selective for the lysophosphatidic acid receptor, $LPA_1$, in treating lung fibrosis We evaluated the *in vitro* and *in vivo* pharmacological properties of the high affinity, selective, oral $LPA_1$-antagonist (4′-{4-[(R)-1-(2-chloro-phenyl)-ethoxycarbonylamino]-3-methyl-isoxazol-5-yl}-biphenyl-4-yl)-acetic acid (AM966).

**Experimental approach:** The potency and selectivity of AM966 for $LPA_1$ receptors was determined *in vitro* by calcium flux and cell chemotaxis assays using recombinant and native cell cultures. The *in vivo* efficacy of AM966 to reduce tissue injury, vascular leakage, inflammation and fibrosis was assessed at several time points in the mouse bleomycin model.

**Key results:** AM966 was a potent antagonist of $LPA_1$ receptors, with selectivity for this receptor over the other LPA receptors. *In vitro*, AM966 inhibited LPA-stimulated intracellular calcium release ($IC_{50}$ = 17 nM) from Chinese hamster ovary cells stably expressing human $LPA_1$ receptors and inhibited LPA-induced chemotaxis ($IC_{50}$ = 181 nM) of human IMR-90 lung fibroblasts expressing $LPA_1$ receptors. AM966 demonstrated a good pharmacokinetic profile following oral dosing in mice. In the mouse, AM966 reduced lung injury, vascular leakage, inflammation and fibrosis at multiple time points following intratracheal bleomycin instillation. AM966 also decreased lactate dehydrogenase activity and tissue inhibitor of metalloproteinase-1, transforming growth factor β1, hyaluronan and matrix metalloproteinase-7, in bronchoalveolar lavage fluid.

**Conclusions and implications:** These findings demonstrate that AM966 is a potent, selective, orally bioavailable $LPA_1$ receptor antagonist that may be beneficial in treating lung injury and fibrosis, as well as other diseases that are characterized by pathological inflammation, oedema and fibrosis.

*British Journal of Pharmacology* (2010) **160,** 1699–1713; doi:10.1111/j.1476-5381.2010.00828.x

**Keywords:** fibrosis; lysophosphatidic acid; $LPA_1$ receptor; idiopathic pulmonary fibrosis (IPF); bleomycin; transforming growth factor β1

**Abbreviations:** BALF, bronchoalveolar lavage fluid; BID, twice a day; CHO, Chinese hamster ovary; CTGF, connective tissue growth factor; DMEM, Dulbecco's modified Eagle's medium; DMSO, dimethyl sulfoxide; ECM, extracellular matrix; EMEM, Eagle's minimum essential medium; FBS, foetal bovine serum; H&E, haematoxylin and eosin; HBSS, Hank's buffered salt solution; HEK, human embryonic kidney; IPF, idiopathic pulmonary fibrosis; LDH, lactate dehydrogenase; LPA, lysophosphatidic acid; MMP-7, matrix metalloproteinase-7; PBS, phosphate buffered saline; PDGF, platelet derived growth factor; TGFβ-1, transforming growth factor β-1; TIMP-1, tissue inhibitor of metalloproteinase-1; UUO, unilateral ureteral obstruction

## Introduction

Idiopathic pulmonary fibrosis (IPF) is one of the most common forms of interstitial lung disease and is characterized by alveolar damage and exaggerated scar tissue production that results in fibrous obliteration of lung parenchyma and subsequent lung dysfunction (Wilson and Wynn, 2009). Currently, 5 million people worldwide are affected by IPF with over 200 000 patients in the United States and the median survival time for IPF patients is approximately 3–5 years from the time of diagnosis (Raghu *et al.*, 2006). Despite its prevalence, there are currently no therapies available to halt or reverse the progression of IPF and there are no Food and Drug Administration-approved courses of treatment. Thus, there is

Correspondence: James Swaney, Amira Pharmaceuticals, 9535 Waples St., San Diego, CA 92121, USA. E-mail: james.swaney@amirapharm.com
Received 9 December 2009; revised 10 March 2010; accepted 16 March 2010

a large, unmet medical need for new therapeutic strategies to treat IPF and other diseases that involve pathological tissue fibrosis.

IPF is believed to result from an abnormal wound-healing response following alveolar injury. In this setting, the primary effector cell, the myofibroblast, produces excess scar tissue which leads to dramatic changes in lung architecture and deleterious effects on lung function (Selman and Pardo, 2002). Myofibroblasts are phenotypically differentiated mesenchymal cells that contain a contractile apparatus of α-smooth muscle actin-containing microfilaments and exhibit increased collagen production capacity (Swaney *et al*., 2005). Although myofibroblasts were initially believed to derive solely from resident lung fibroblasts (Gabbiani *et al*., 1971), recent studies have suggested that myofibroblasts can also originate from bone marrow-derived fibroblast precursor cells called 'fibrocytes' (Andersson-Sjoland *et al*., 2008) and from mesenchymal transformation of alveolar epithelial cells (Willis *et al*., 2005; Tanjore *et al*., 2009). Regardless of their cellular origin, myofibroblasts are the main effector cell in IPF and other fibrotic diseases (Scotton and Chambers, 2007). The formation and the subsequent fibrogenic capacity of myofibroblasts are regulated by mechanical stimuli, as well as by the biochemical milieu (Tomasek *et al*., 2002). In response to tissue injury, elevated local and/or circulating concentrations of growth factors, such as platelet-derived growth factor (PDGF) and cytokines [transforming growth factor β (TGFβ) and interleukins] promote myofibroblast transformation of precursor cell populations with subsequent increases in tissue fibrosis (Wynn, 2008).

Lysophosphatidic acid (LPA) is a bioactive lysophospholipid that regulates numerous aspects of cellular function and has been recognized as a novel mediator of wound healing and tissue fibrosis (Watterson *et al*., 2007). LPA signals through a family of at least five G protein-coupled receptors, designated $LPA_{1–5}$ (nomenclature follows Alexander *et al*., 2009; Anliker and Chun, 2004). Several studies have recently linked $LPA_1$ receptors to the pathogenesis of lung and kidney fibrosis and identified these receptors as a potential clinical target for IPF (Ley and Zarbock, 2008; Tager *et al*., 2008). Tager *et al*. showed that LPA levels were increased in the bronchoalveolar lavage fluid (BALF) of IPF patients. In addition, $LPA_1$ receptors were the most highly expressed LPA receptors in lung fibroblasts isolated from IPF patients and BALF-stimulated chemotaxis by these cells was inhibited by an $LPA_{1,3}$ receptor-selective antagonist. Consistent with these findings, $LPA_1$ receptor null mice were protected from bleomycin-induced lung fibrosis via a reduction in vascular leakage and fibroblast recruitment (Tager *et al*., 2008). In a renal fibrosis model, tubulointerstitial fibrosis was reduced in $LPA_1$ receptor knockout mice following unilateral ureteral obstruction (UUO) (Pradere *et al*., 2007). In this same study, an $LPA_{1,3}$ receptor antagonist recapitulated the decrease in renal fibrosis and inhibited mRNA expression of TGFβ and connective tissue growth factor (CTGF) (Pradere *et al*., 2007), suggesting that these fibrogenic factors act downstream of $LPA_1$ and/or $LPA_3$ receptors.

In this study, we characterized the *in vitro* and *in vivo* pharmacological properties of an oral, high affinity, selective $LPA_1$ receptor antagonist (AM966) and assessed the efficacy of AM966 in a mouse model of lung fibrosis induced by bleomycin. Furthermore, we examined the ability of AM966 to modulate cytokine and protease concentrations in the lung in order to elucidate the potential mechanism by which $LPA_1$ receptor antagonism inhibited lung inflammation and fibrosis. Here we report that AM966 exhibited good oral bioavailability and pharmacokinetics in rats and mice. AM966 reduced tissue injury, vascular leakage, inflammation and fibrosis at several time points in the bleomcyin lung fibrosis model and decreased concentrations of several pro-fibrotic and pro-inflammatory cytokines in BALF. These data establish the $LPA_1$ receptor antagonist as a potential anti-fibrotic therapy and pave the way for the clinical development of 'first in class' molecules that treat IPF via blockade of $LPA_1$ receptors.

## Methods

*Cells/recombinant expression*

A2058 human melanoma cells were obtained from ATCC and cultured in Dulbecco's modified Eagle's medium (DMEM) containing 10% FBS. IMR-90 human foetal lung fibroblasts were obtained from ATCC and cultured in Eagle's minimum essential medium (EMEM) containing 10% foetal bovine serum (FBS). B103 rat neuroblastoma cells were obtained from Jerold Chun at The Scripps Research Institute and cultured in DMEM containing 10% FBS. Human and mouse $LPA_1$ and human $LPA_3$ receptors were stably expressed in Chinese hamster ovary (CHO) cells and cultured in F12 media containing 10% FBS and 1 mg/mL hygromycin B. Mouse $LPA_3$ receptors were stably expressed in human embryonic kidney (HEK) cells and cultured in DMEM containing 10% FBS and 200 μg/mL hygromycin B. Human and mouse $LPA_2$ and human and mouse $LPA_5$ receptors were transiently expressed in rat neuroblastoma B103 cells using Lipofectamine™ 2000 (Invitrogen, Carlsbad, CA, USA) following the manufacturers' instruction. Human $LPA_4$ receptors were expressed stably in rat neuroblastoma B103. Briefly, on the day before the assay, 30 000–35 000 cells per well were seeded together with 0.2 μL lipofectamine 2000 and 0.2 μg expression vector in 96-well Poly-D-Lysine coated black-wall clear-bottom plates (BD BioCoat, Franklin Lakes, NJ, USA) in DMEM + 10% FBS. Following an overnight culture, cells were washed once with phosphate buffered saline (PBS) then cultured in serum-free media for 4 h prior to dye loading.

*Calcium flux*

Stably expressing cells were plated in 96-well Poly-D-Lysine coated black-wall clear-bottom plates (BD BioCoat) at a density of 20 000–40 000 cells per well and cultured overnight in complete media. The following day, cells were washed once with PBS then cultured in 75 μL serum-free media either overnight (for the stably expressing cells) or 4 h (for the transient tranfectants) prior to dye loading. On the day of the assay, cells were loaded for 1 h at 37°C with 100 μL FLIPR Calcium 4 dye (Molecular Devices, Sunnyvale, CA, USA) prepared in Hank's buffered salt solution (HBSS) supplemented with 20 mM HEPES (pH 7.4), 2 mM probenecid and 0.3% fatty-acid-free human serum albumin. 25 μL test com-

pounds (prepared in 1% DMSO) were added to each well and incubated at room temperature for 30 min. After 15 s of baseline measurement, 50 µL of 50 nM LPA [prepared in HBSS supplemented with 20 mM HEPES (pH 7.4), and 0.3% fatty-acid-free human serum albumin] was added. Intracellular calcium mobilization was measured using the FLEXstation III (Molecular Devices).

*Cell chemotaxis*

Neuroprobe ChemoTx® System plates (8 µm pore size, 5.7 mm diameter sites; Gaithersburg, MD, USA) were coated on both sides with 20 µL of 0.001% fibronectin and allowed to dry. The bottom wells were loaded with 100 nM LPA or vehicle in DMEM containing 0.1% fatty acid free bovine serum albumin (BSA). A2058 human melanoma cells and IMR-90 human lung fibroblasts were serum starved for 24 h, harvested and resuspended in DMEM containing 0.1% fatty acid free BSA. CHO cells over-expressing mouse $LPA_1$ receptors were serum starved for 24 h, harvested and resuspended in F12K media containing 0.2% fatty acid free BSA. The cells were incubated with inhibitor or vehicle for 15 min at 37°C before applying 25 000 (A2058 and CHO) or 50 000 (IMR-90) cells to the upper portion of the ChemoTx® plate. The plates were incubated for 3 h (A2058), 4 h (CHO) or 16–18 h (IMR-90) at 37°C. Cells were removed from the upper portion of the filter by rinsing with PBS and scraping. The filter was allowed to dry before staining with the HEMA 3 Staining System (Fisher Scientific, Pittsburg, PA, USA). The absorbance of the filter was then read at 590 nm and calculation of the cell number was made from the standard curve.

*Pharmacokinetics*

The oral exposure of AM966 was determined in fasted mice. Animals received AM966 (10 $mg \cdot kg^{-1}$) in vehicle (water) by oral gavage and were then killed by $CO_2$ inhalation at 1, 2, 4, 8 and 24 h post dose ($n$ = 2 animals per time point for each test compound). Blood (approximately 300 µL) was collected via cardiac puncture into EDTA-containing tubes and centrifuged at 1450× $g$ for 10 min. The plasma was removed and analysed for AM966 content by liquid chromatography-mass spectrometry (LCMS). Briefly, known amounts of AM966 were added to thawed mouse plasma to yield a concentration range from 0.8 to 4000 $ng \cdot mL^{-1}$. Mouse plasma samples were precipitated using acetonitrile (1:4, v:v) containing the internal standard buspirone. A 10 µL aliquot of the analyte mixture was injected using a Leap PAL autosampler (Leap Technologies, Carrboro, NC, USA). Analyses were performed using an Agilent Zorbax SB-C8 column (Agilent Technologies, Santa Clara, CA, USA) (2.1 × 50 mm; 5 µm) linked to a Shimadzu LC-10AD VP with SCL-10A VP system controller (Shimadzu Scientific Instruments, Colombia, MD, USA). Tandem mass spectrometric detection was carried out on a PE Sciex API3200 (Applied Biosystems, Foster City, CA, USA) in the positive ion mode (ESI) by multiple reaction monitoring. The calibration curves were constructed by plotting the peak–area ratio of analysed peaks against known concentrations. The lower limit of quantitation was 0.8 $ng \cdot mL^{-1}$. The data were subjected to linear regression analysis with $1/x^2$ weighting.

*Bleomycin model*

Female C57BL/6 mice (Harlan, San Francisco, CA, USA; 20–25 g) were housed at four per cage, given free access to food and water and allowed to acclimatize for at least 7 days prior to test initiation. After the habituation phase, mice were lightly anaesthetized with isoflurane (5% in 100% $O_2$) and treated with bleomycin sulfate (Blenoxane, Henry Schein, Melville, NY, USA; 1.5–5 $units \cdot kg^{-1}$) via intratracheal instillation. Mice were returned to their cages and monitored daily for the duration of the experiment. Vehicle (water), AM966, and Pirfenidone were delivered twice daily (BID) and dexamethasone was delivered once daily (QD) over the course of each study. All compounds were delivered by oral gavage. At 3, 7, 14 or 28 days after bleomycin instillation, animals were killed with inhaled isoflurane. Following death, mice were intubated with a 20 gauge angiocatheter attached to a 1 mL syringe. Lungs were lavaged with saline (2 × 0.75 mL) to obtain BALF and cells and then the lungs were removed and fixed in 10% neutral buffered formalin for subsequent histopathological analysis.

*BALF analysis*

BALF was centrifuged for 10 min at 800× $g$ to pellet the cells and the BALF supernatant was removed and frozen at –80°C for subsequent protein analysis using the DC protein assay kit (Biorad, Hercules, CA, USA) and soluble collagen analysis. BALF was analysed for concentrations of inflammatory, profibrotic and tissue injury biomarkers including tissue inhibitor of metalloproteinase-1 (TIMP-1), TGFβ1, hyaluronan and matrix metalloproteinase (MMP)-7, and lactate dehydrogenase (LDH) activity, using commercially available kits. The cell pellet was re-suspended in PBS/0.1% BSA. Total cell counts were obtained using a Hemavet haematology system (Drew Scientific, Wayne, PA, USA) and differential cells counts were determined using Shandon cytospin (Thermo Scientific, Waltham, MA, USA). All counts were expressed as $cell \cdot mL^{-1}$.

*Histopathology*

Lung tissue was stained using H&E and Masson's Trichrome and the severity of lung fibrosis was determined by semiquantitative histopathological scoring (Ashcroft *et al*., 1988) using light microscopy (100× magnification). To do this, lung fibrosis was scored on a scale of 0–8 by examining 45 randomly chosen fields (5 lobes / mouse × 3 sections / lobe × 3 fields / section) for each mouse. As defined by Ashcroft *et al*. (1988) the criteria for grading lung fibrosis were as follows: grade 0 = normal lung; grade 1 = minimal fibrous thickening of alveolar or bronchiolar walls; grade 3 = moderate thickening of walls without obvious damage to lung architecture; grade 5 = increased fibrosis with definite damage to lung structure and formation of fibrous bands or small fibrous masses; grade 7 = severe distortion of structure and large fibrous areas; and grade 8 = total fibrous obliteration of the fields. If there was any difficulty in deciding between two odd-numbered categories, the field was given the intermediate even-numbered score.

*Collagen quantification in BALF*

Soluble collagen concentrations in BALF were assessed using a modification of previously described methods (Jankov *et al*.,

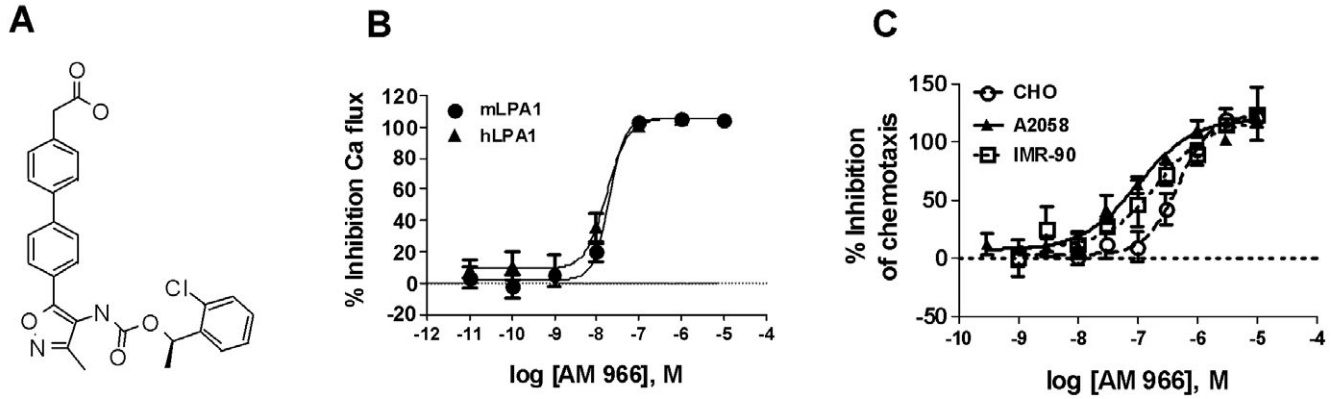


**Figure 1** Pharmacological characterization of AM966 as an $LPA_1$ receptor antagonist. (A) Structure of AM966. (B) Inhibition of LPA-stimulated intracellular calcium release from CHO cells stably expressing the mouse (mLPA1) and human $LPA_1$ (hLPA1) receptors. CHO cells were pre-treated with increasing concentrations of AM966 for 30 min and then stimulated with LPA (10–30 nM) and calcium release was measured. (C) AM966-mediated inhibition of cell chemotaxis of human A2058 melanoma cells ($IC_{50}$ = 138 nM), IMR-90 human lung fibroblasts ($IC_{50}$ = 181 nM) and CHO mLPA$_1$ cells ($IC_{50}$ = 469 nM). LPA, lysophosphatidic acid; CHO, Chinese hamster ovary.

**Table 1** Inhibition of LPA-stimulated intracellular calcium release from cells expressing the human or mouse $LPA_{1-5}$ receptors

| | *AM966 $IC_{50}$ (μM)* | | | | |
|---|---|---|---|---|---|
| | *$LPA_1$* | *$LPA_2$* | *$LPA_3$* | *$LPA_4$* | *$LPA_5$* |
| Human | 0.017 ± 0.002 (*n* = 8) | 1.7 (*n* = 1) | 1.6 ± 0.1 (*n* = 12) | 7.7 (*n* = 1) | 8.6 (*n* = 2) |
| Mouse | 0.019 ± 0.002 (*n* = 6) | ~25 (*n* = 1) | 0.17 ± 0.03 (*n* = 8) | ND | ~23 (*n* = 1) |

Data represent the mean ± standard error of the mean.
LPA, lysophosphatidic acid; ND, not determined.

2002). Briefly, BALF samples (20–50 μL in 1 mL of 0.5 M acetic acid) and collagen type I standards (0–500 μg·mL$^{-1}$) in 1 mL acetic acid (0.5 M) were added to an equal volume of Sirius Red (direct red 80; 120 μg·mL$^{-1}$ in 0.5 M acetic acid). Samples were incubated at room temperature for 30 min with gentle agitation, centrifuged at 10 000× *g* for 10 min and the absorbance of 200 μL of sample supernatant was read at 540 nm and plotted against standards with a known concentration of collagen type I.

*Statistical analyses*

Values are expressed as mean ± standard error of the mean. Groups were compared using one- and two-way analysis of variance with Bonferroni and Dunnett's, *post hoc*, multiple comparison tests. Kaplan-Meier curves were compared using a log-rank (Mantel–Cox) test. Statistical significance was set at $P < 0.05$. Statistical comparisons and graphical representations were performed using GraphPad Prism 5.0 (GraphPad Software, San Diego, CA, USA).

*Materials*

LPA (18:1 LPA 1-oleoyl-2-hydroxy-*sn*-glycero-3-phosphate, sodium salt) was purchased from Avanti Polar Lipids (Alabaster, AL, USA). AM966 and pirfenidone (5-methyl-1-phenylpyridin-2-one) were synthesized at Amira Pharmaceuticals (San Diego, CA, USA). Pirfenidone synthesized at Amira was of identical chemical purity to material obtained commercially from 3B Pharmachem (Wuhan, Libertyville, IL, USA) International Inc., as determined by NMR and LCMS. Bleomycin sulphate (Blenoxane) was purchased from Henry Schein (Melville, NY). Total TGFβ$_1$ and TIMP-1 kits were obtained from R&D Systems (Minneapolis, MN, USA). Hyaluronan kits were obtained from Echelon Biosciences (Salt Lake City, UT, USA). MMP-7 kits were obtained from USCN Life Science Inc. (Wuhan, China). LDH activity assay kits, dexamethasone, direct red 80 and rat tail collagen were purchased from Sigma Aldrich (St. Louis, MO, USA).

## Results

*AM966 is a selective $LPA_1$ receptor antagonist*

AM966 (Figure 1A) was synthesized and its potency for $LPA_1$ receptors and selectivity for the different LPA receptors was determined by Ca flux assays using cells over-expressing human and mouse $LPA_{1-5}$ receptors. AM966 inhibited LPA-stimulated intracellular calcium release from CHO cells stably expressing human and mouse $LPA_1$ receptors (Figure 1B; Table 1). As shown in Table I, AM966 was 100-fold and 10-fold more selective in human and mouse cells, respectively, for $LPA_1$ relative to the other LPA receptors. AM966 was also evaluated for inhibition of LPA-induced chemotaxis in A2058 human melanoma cells and IMR-90 human lung fibroblasts endogenously expressing $LPA_1$ receptors and in CHO cells stably expressing mouse $LPA_1$ receptors. As shown in

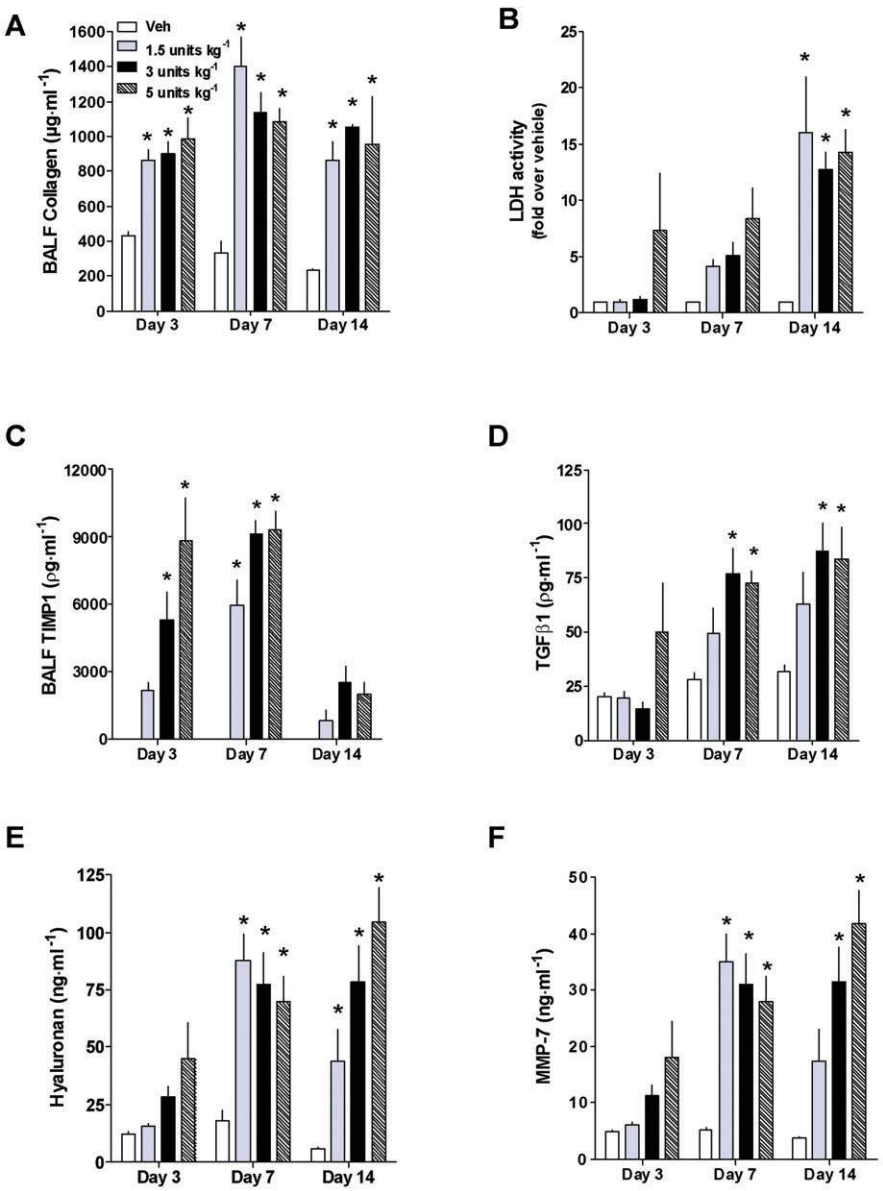


**Figure 2** Time course of inflammatory, fibrotic and cell death markers in the mouse bleomycin model. Effects of bleomycin on (A) soluble collagen (B) LDH activity (cell death marker) and (C) TIMP-1 (D) TGFβ1 (E) hyaluronan and (F) MMP-7 concentrations in BALF at several time points (3, 7 and 14 days) following intratracheal instillation of bleomycin (1.5, 3, and 5 units·kg$^{-1}$). Data represent the mean ± standard error of the mean of $n \geq 4$ mice per group. * denotes a significant increase ($P < 0.05$) compared to vehicle at each time point. LDH, lactate dehydrogenase; TGFβ-1, transforming growth factor β-1; TIMP-1, tissue inhibitor of metalloproteinase-1; MMP-7, matrix metalloproteinase-7; BALF, bronchoalveolar lavage fluid; Veh, vehicle.

Figure 1C, AM966 inhibited LPA$_1$-mediated chemotaxis of human A2058 melanoma cells ($IC_{50}$ = 138 ± 43 nM), IMR-90 human lung fibroblasts ($IC_{50}$ = 182 ± 86 nM) and CHO mLPA$_1$ cells ($IC_{50}$ = 469 ± 54 nM).

*Time- and dose-dependent effects of bleomycin on lung markers of injury and fibrosis*

In order to characterize the time- and dose-dependent effects of bleomycin on biochemical markers of lung injury and fibrosis, we measured soluble collagen, LDH activity and TIMP-1, TGFβ1, hyaluronan and MMP-7 concentrations in BALF at several points (3, 7 and 14 days) following intratracheal instillation of bleomycin (1.5, 3, and 5 units·kg$^{-1}$). BALF collagen concentrations were increased at all times and in response to all doses of bleomycin (Figure 2A). Analysis of LDH activity revealed very little change at the 3 day point, except for the 5 units·kg$^{-1}$ bleomycin dose (Figure 2B). However, by days 7 and 14, LDH activity was increased at all bleomycin doses and showed an approximately 15-fold elevation in activity by day 14. The bleomycin-induced changes in soluble collagen prompted us to examine BALF concentrations of several well-known pro-fibrotic mediators. Among these factors, the matrix metalloproteinase inhibitor, TIMP-1, was elevated in the early window at days 3 and 7 following bleomycin injury (Figure 2C) but decreased dramatically by

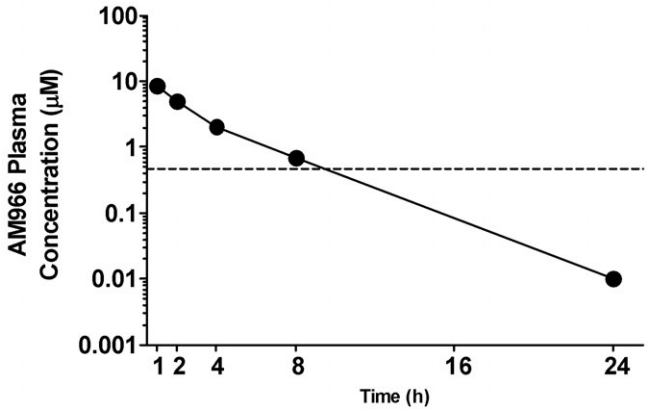


**Figure 3** Time-concentration profile for AM966. Fasted mice ($n = 2$) were dosed with AM966 and blood was sampled at 1, 2, 4, 8 and 24 h after oral dosing (10 mg·kg$^{-1}$). The dashed line in Figure 3 represents the $IC_{50}$ value for AM966-mediated inhibition of cellular chemotaxis by Chinese hamster ovary cells expressing recombinant mouse $LPA_1$ receptors (See Figure 1D).

day 14. In contrast, TGFβ1, hyaluronan and MMP-7 were only slightly elevated on day 3 but dramatically increased between days 7 and 14 (Figure 2D–F). Notably, 25% mortality was observed at the high (5.0 units·kg$^{-1}$) bleomycin dose, whereas all mice survived at the lower (1.5 and 3.0 units·kg$^{-1}$) doses in this study. These data demonstrate that several biochemical mediators of tissue inflammation and fibrosis are elevated in this model and these factors correlate with increased lung injury and fibrosis following bleomycin administration.

*AM966 demonstrates a good pharmacokinetic profile in vivo*

AM966 was given orally to non-fasted mice at 10 mg·kg$^{-1}$ and plasma concentrations were measured over a 24 h period (Figure 3). AM966 peaked within 1 h to a concentration of 9 μM and decreased to 10 nM over a 24 h period. The dashed line in Figure 3 represents the $IC_{50}$ value of 469 nM for AM966-mediated inhibition of chemotaxis by CHO cells expressing recombinant mouse $LPA_1$ (see Figure 1C). Based on these data, a single 10 mg·kg$^{-1}$ oral dose of AM966 was not sufficient to maintain plasma drug concentrations above the $IC_{50}$ for chemotaxis for 24 h. Therefore, in all bleomycin studies we used twice a day (BID) dosing to attain full drug coverage over a 24 h period.

*The $LPA_1$ receptor antagonist, AM966, reduces vascular leakage, fibrosis and inflammation in the acute (3–7 day) window after bleomycin lung injury*

Increases in vascular permeability and inflammation are observed as early as day 3 after bleomycin lung injury (Izbicki *et al*., 2002; Tager *et al*., 2008) and by day 7, tissue fibrosis is detectable (Cuzzocrea *et al*., 2007). As early as day 3 (Figure 4), AM966 decreased ($P < 0.05$) BALF protein concentrations in a dose-dependent manner, resulting in 43% reduction at the 30 mg·kg$^{-1}$ dose (Figure 4A). This reduction is comparable with that observed in the $LPA_1$ receptor knockout mouse (Tager *et al*., 2008), demonstrating full antagonism of $LPA_1$ receptors by AM966 at 30 mg·kg$^{-1}$. A similar reduction in BALF cells was observed in response to AM966, albeit this decrease was not statistically significant (Figure 4B). AM966 also inhibited the bleomycin-induced lung damage as demonstrated by the decrease in LDH activity at 10 and 30 mg·kg$^{-1}$ (Figure 4C). Based on these findings at day 3, a 7 day study was conducted in which the dose range was expanded to include a 1 mg·kg$^{-1}$ AM966 dose (Figure 5). Consistent with the 3 day results, AM966 significantly reduced BALF protein at the 10 and 30 mg·kg$^{-1}$ doses (Figure 5A). In addition, AM966 reduced BALF collagen and total TGFβ concentrations (Figure 5B,C) in the lung. In order to assess the effects of AM966 on tissue fibrosis at day 7, mouse lungs were stained with Trichrome (Figure 5D). Compared to vehicle controls (Figure 5D, panel a.), increased tissue remodelling and fibrosis were observed in bleomycin-instilled mice (Figure 5D, panel b.). In contrast, lungs from mice treated with AM966 (30 mg·kg$^{-1}$) exhibited a decrease in tissue fibrosis and maintenance of normal lung architecture (Figure 5D, panel c.). Furthermore, the decrease in lung leakage and fibrosis at day 7 was accompanied by a lowering of total BALF cells, with this reduction comprised primarily of macrophages and neutrophils (Figure 5E). Thus, $LPA_1$ receptor antagonism decreases vascular permeability, inflammation and fibrosis in the early (3–7 day) window after bleomycin-induced lung injury.

*AM966 inhibits lung fibrosis, maintains mouse body weight and decreases lung inflammation 14 days after bleomycin lung injury*

To assess the therapeutic potential of $LPA_1$ antagonism in treating lung fibrosis at later time points, we examined the anti-fibrotic activity of AM966 14 days after bleomycin (1.5 unit·kg$^{-1}$) lung injury. Day 14 after a single intratracheal instillation of bleomycin is reported to be the most appropriate time point for assessing lung fibrosis in this model (Izbicki *et al*., 2002). Histological examination of mouse lungs following bleomycin instillation revealed significant damage to the lung tissue, including thickening of the alveolar septae, alveolar inflammation and fibrous obliteration of the peribronchiolar and parenchymal regions (Figure 6A, panel b.), compared to the vehicle group (Figure 6A, panel a.). No reduction in lung fibrosis was observed in response to either the dexamethasone (Figure 6A, panel c) or low dose AM966 (10 mg·kg$^{-1}$; Figure 6A, panel d.). However, AM966 at 30 and 60 mg·kg$^{-1}$ dramatically reduced lung tissue remodelling and fibrosis (Figure 6A, panels e–f.) so that lung architecture in these groups was similar to that of the vehicle group (Figure 6A, panel a.). The reduction in fibrosis was confirmed by quantitative analysis of BALF collagen concentrations (Figure 6B) and histopathological scoring of lung fibrosis (Figure 6C), according to Ashcroft *et al*. (1988). Consistent with the reduction in lung pathology, the bleomycin-induced body weight loss was inhibited in the 30 and 60 mg·kg$^{-1}$ treatment groups (Figure 6D) demonstrating an enhanced overall state of health.

Pulmonary inflammation is a precipitating or complicating component of many fibrotic lung diseases and very few clinical treatment strategies address both the inflammatory and fibrotic components of IPF. For this reason, we examined the role of $LPA_1$ receptors in inflammatory cell infiltration in the lungs after bleomycin injury (Figure 6E). Similar to previous

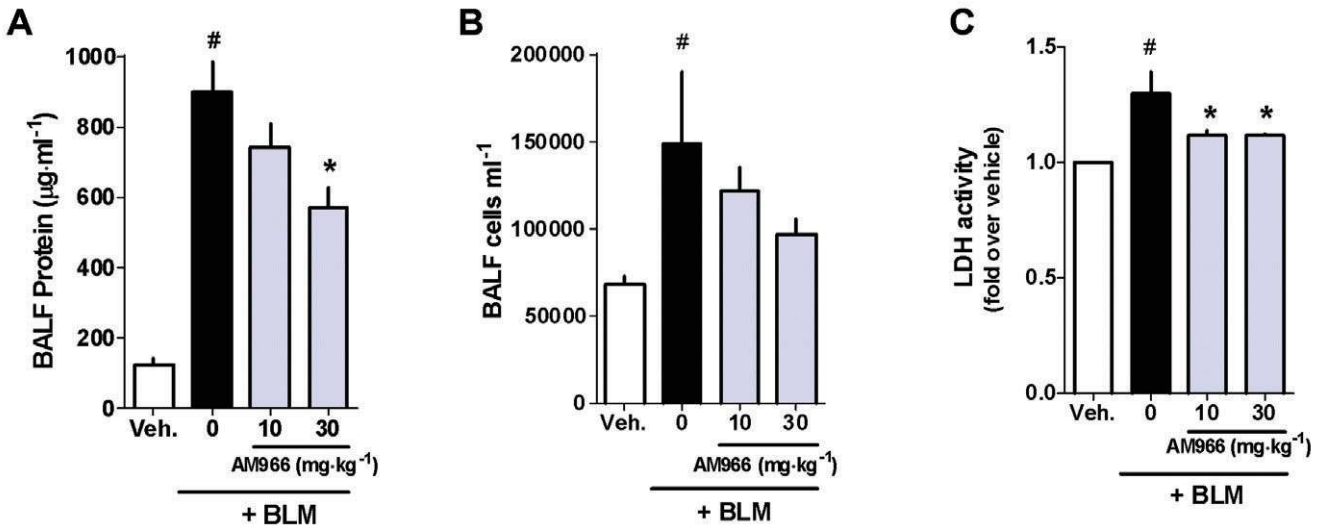


**Figure 4** AM966 reduces vascular leakage, inflammation and lung injury and inflammation in a 3 day bleomycin model. Mice were given intratracheal bleomycin sulfate (BLM; 1.5 units·kg$^{-1}$) or saline vehicle (Veh.), followed by oral (gavage) administration of AM966 (10 and 30 mg·kg$^{-1}$, BID) for a period of 3 days. BALF was isolated and analysed for changes in (A) total protein, (B) inflammatory cells, and (C) LDH activity. Data represent the mean ± standard error of the mean of $n = 5$–7 mice per group. # denotes a significant increase ($P < 0.05$) compared to vehicle control. * denotes a significant decrease ($P < 0.05$) compared to BLM. BID, twice a day; BALF, bronchoalveolar lavage fluid; LDH, lactate dehydrogenase.

reports, dexamethasone inhibited lung inflammation, as indicated by a reduction in the total number of inflammatory cells, as well as specific decreases in macrophages, neutrophils and lymphocytes in the BALF. The fact that dexamethasone had an anti-inflammatory effect but did not affect lung fibrosis suggests that, at least in our hands, decreasing inflammation is not sufficient to decrease fibrosis. AM966 at 10 mg·kg$^{-1}$ had no effect on total cells, macrophages, neutrophils or lymphoctyes. In contrast, at the 30 and 60 mg·kg$^{-1}$ doses, AM966 reduced total and differential cell counts to a greater extent than dexamethasone. These data demonstrate that LPA$_1$ receptor antagonism limits the infiltration of inflammatory cells in the lung following tissue injury.

*AM966 reduces vascular leakage, tissue injury and pro-fibrotic cytokine production in the 14 day bleomycin study*

Mice lacking LPA$_1$ receptors exhibit decreased pulmonary vascular leakage following bleomycin injury, which is believed to contribute to a reduction in lung damage (Tager *et al.*, 2008). In order to understand the mechanism by which LPA$_1$ receptor blockade inhibits lung injury and fibrosis (see Figures 4–6), we examined the effects of AM966 on BALF protein, LDH activity and BALF concentrations of various inflammatory and pro-fibrotic mediators. In the 14 day bleomycin model, AM966 attenuated vascular leakage, as shown by a significant ($P < 0.05$) reduction in BALF protein (Figure 7A). In addition, AM966-treated animals showed decreased LDH activity in BALF (Figure 7B), indicative of a decrease in lung tissue injury. AM966 significantly reduced BALF concentrations of TIMP-1, TGFβ1, hyaluronan and MMP-7 (Figure 7C–F), factors that are linked to lung inflammation and fibrosis (Bjermer *et al.*, 1989; Broekelmann *et al.*, 1991; Swiderski *et al.*, 1998; Rosas *et al.*, 2008). Dexamethasone (1 mg·kg$^{-1}$) had no effect on BALF protein or LDH activity and actually increased BALF concentrations of TIMP-1, TGFβ1 and hyaluronan (Figure 7A–E). However, a reduction in MMP-7 by dexamethasone was observed (Figure 7F). When combined with the 3 and 7 day bleomycin data (Figure 4), these findings provide mechanistic insight into the ability of AM966 to attenuate lung tissue damage, inflammation and fibrosis at multiple time points after lung insult.

*AM966 demonstrates greater efficacy compared to pirfenidone in the 14 day bleomycin model*

Pirfenidone is an anti-fibrotic agent that has recently been approved for IPF in Japan and is under regulatory review in the United States. Therefore, we compared the efficacy of AM966 (30 mg·kg$^{-1}$, BID) to that of pirfenidone (20, 100 and 400 mg·kg$^{-1}$, BID) 14 days after bleomycin (3.0 units·kg$^{-1}$) challenge. As shown in Figure 8, lung fibrosis (Figure 8A, panel c.) was once again reduced by AM966, compared to the bleomycin-only group (Figure 8A, panel b.). Remarkably, no therapeutic benefit was observed in pirfenidone-treated mice (Figure 8A, panels d–f.). Consistent with these findings, both BALF collagen concentrations (Figure 8B) and tissue fibrosis scores (Figure 8C) were significantly reduced by AM966, whereas pirfenidone had no effect when compared to mice treated with bleomycin alone. Although the mouse body weight loss in the AM966 group was similar to that observed at this increased dose of bleomycin (3.0 unit·kg$^{-1}$; see Figure 6D for comparison), a decrease in body weight was seen in response to the 100 mg·kg$^{-1}$ and 400 mg·kg$^{-1}$ pirfenidone doses (Figure 8D). This same trend was observed for BALF protein, LDH activity and TIMP-1, which were all decreased by AM966, whereas pirfenidone showed little or no therapeutic benefit (Figure 8E–G). Thus, AM966 demonstrates greater efficacy than pirfenidone at reducing lung

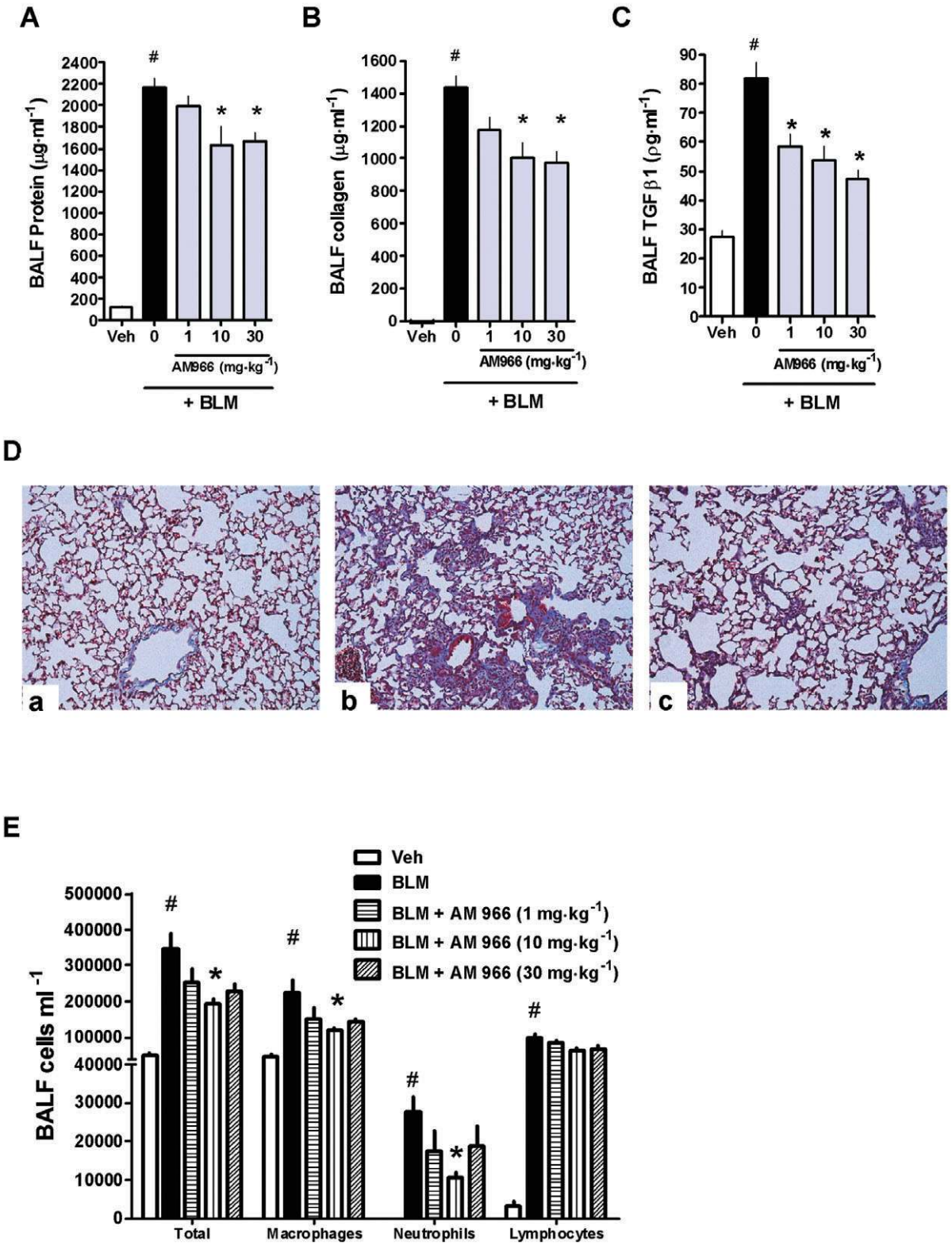


**Figure 5** AM966 reduces vascular leakage and fibrosis in a 7 day bleomycin model. Mice were given intratracheal bleomycin sulfate (BLM; 3.0 units·kg$^{-1}$) or saline vehicle (Veh.), followed by oral (gavage) administration of AM966 (1, 10 and 30 mg·kg$^{-1}$, BID) for a period of 7 days. BALF was isolated and analysed for changes in (A) total protein, (B) collagen, (C) total (TGF$\beta_1$). (D) Representative histopathological images (100× magnification; trichrome staining) are shown of the lungs of mice treated with (a) vehicle, (b) BLM or (c) BLM + AM966 (30 mg·kg$^{-1}$, BID). Blue staining denotes regions of fibrosis. (E) Total cellularity was analysed using a Hemavet system and differential cell counts for macrophages, neutrophils and lymphocytes were measured by cytospin in BALF. Data represent the mean ± standard error of the mean of $n$ = 8 mice per group. # denotes a significant increase ($P < 0.05$) compared to vehicle control. * denotes a significant decrease ($P < 0.05$) compared to BLM. BID, twice a day; BALF, bronchoalveolar lavage fluid.

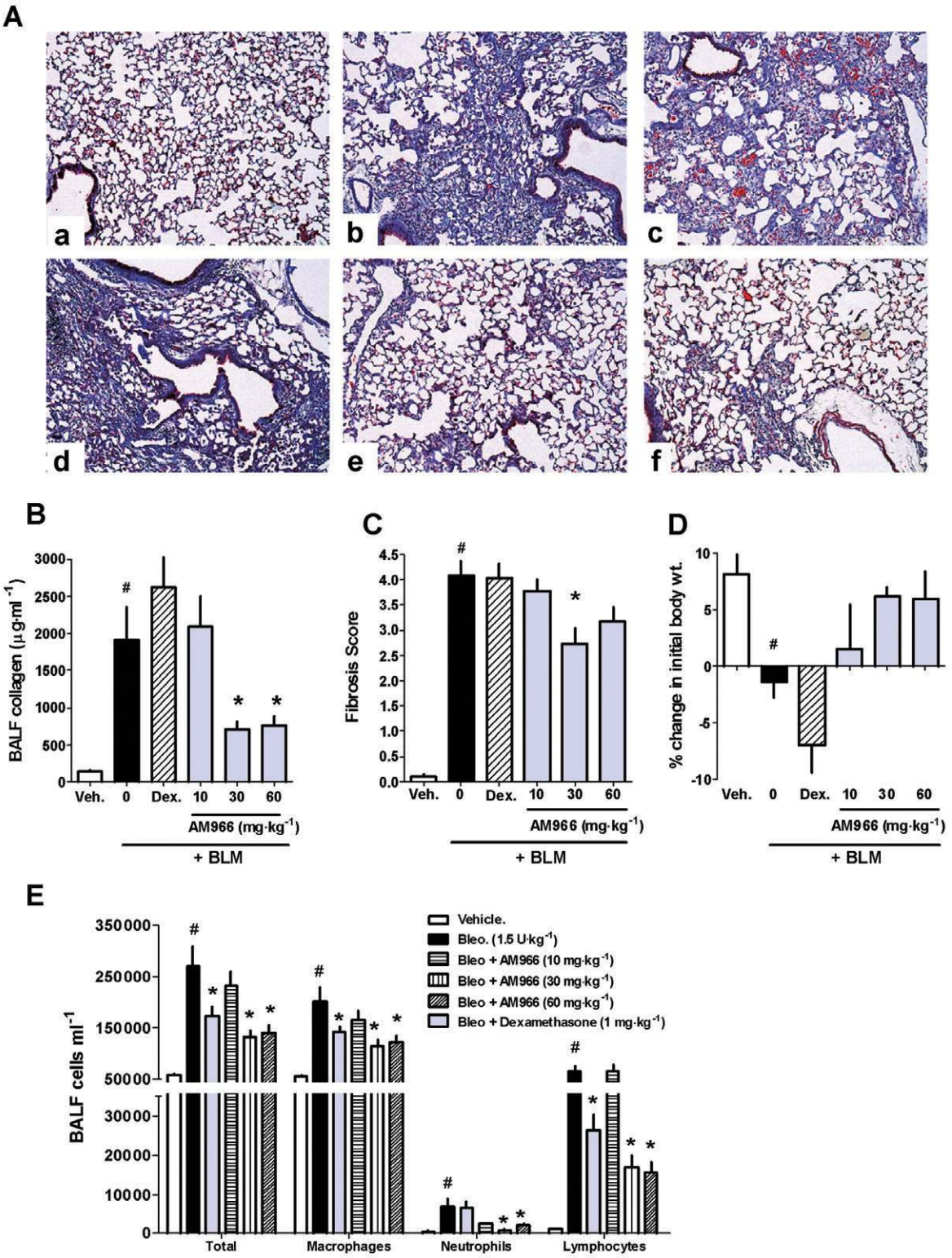


**Figure 6** AM966 inhibits lung fibrosis and maintains body weight 14 days after bleomycin-induced lung injury. Mice were given intratracheal bleomycin sulfate (BLM; 1.5 units·kg$^{-1}$) or saline vehicle (Veh.), followed by oral (gavage) administration of dexamethasone (1 mg·kg$^{-1}$, QD) or AM966 (10, 30 and 60 mg·kg$^{-1}$, BID) for a period of 14 days. (A, a-f) Representative histopathological images (100× magnification; Trichrome staining) are shown of the lungs of mice treated with (a) vehicle, (b) BLM, (c) BLM + dexamethasone (1 mg·kg$^{-1}$, QD), (d) BLM + AM966 (10 mg·kg$^{-1}$, BID), (e) BLM + AM966 (30 mg·kg$^{-1}$, BID) or (f) BLM + AM966 (60 mg·kg$^{-1}$, BID). (B) Soluble collagen in BALF. (C) Histopathological scoring of lung fibrosis. (D) Percentage change in mouse body weight (wt.). (E) Total cellularity and differential cell counts for macrophages, neutrophils and lymphocytes. Data represent the mean ± standard error of the mean of $n = 8$ mice per group. # denotes a significant increase ($P < 0.05$) compared to vehicle control. * denotes a significant decrease ($P < 0.05$) compared to BLM. QD, once a day; BID, twice a day; BALF, bronchoalveolar lavage fluid.

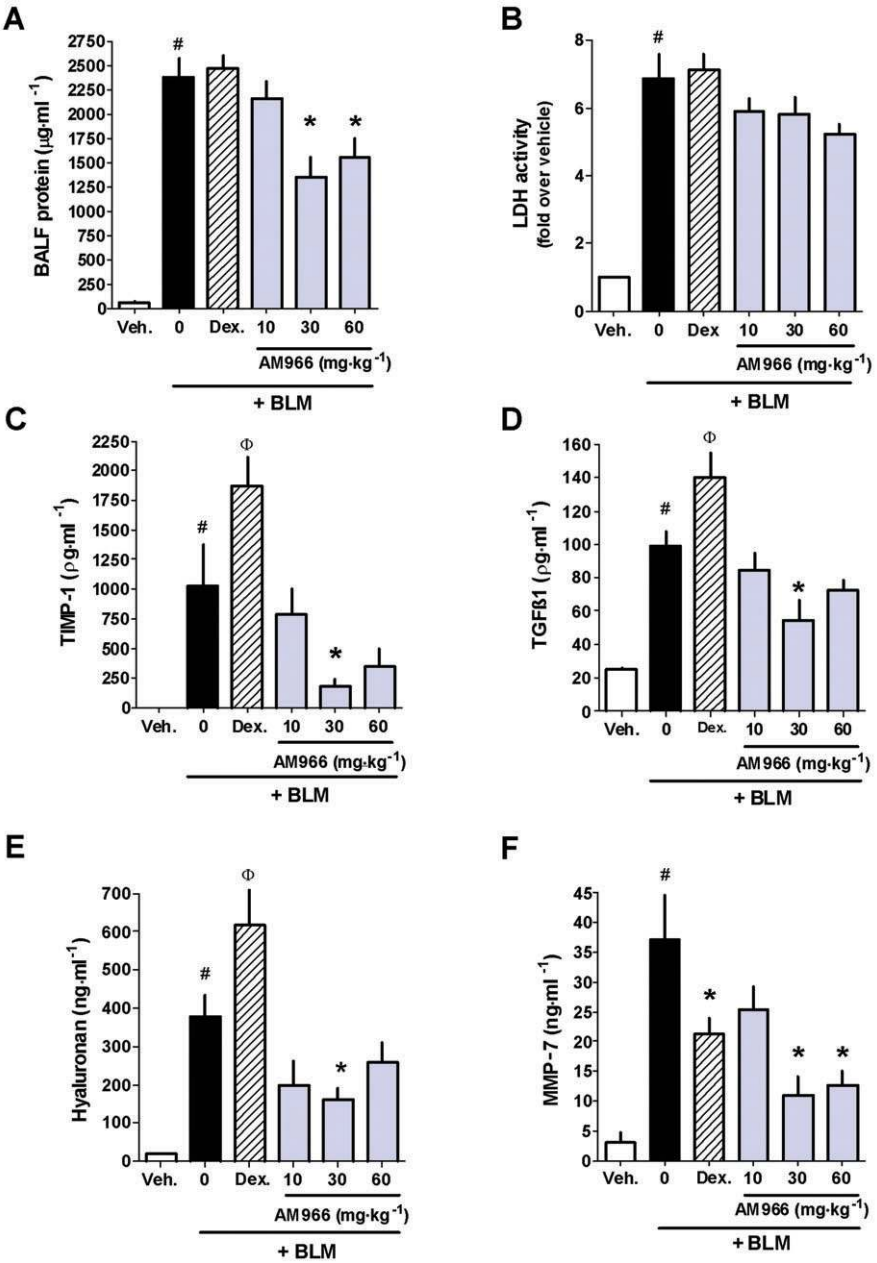


**Figure 7** AM966 reduces vascular leakage, tissue injury and pro-fibrotic cytokine production. Mice were treated in the same manner as described for Figure 6. (A) Total protein (B) LDH activity (cell death marker) and concentrations of the pro-fibrotic factors (C) TIMP-1 (D) TGFβ1 (E) hyaluronan and (F) MMP-7 were analysed using commercially available kits. Data represent the mean ± standard error of the mean of $n$ = 8 mice per group. # denotes a significant increase ($P < 0.05$) compared to vehicle control. Φ denotes a significant ($P < 0.05$) increase compared to BLM. * denotes a significant decrease ($P < 0.05$) compared to BLM. LDH, lactate dehydrogenase; TIMP-1, tissue inhibitor of metalloproteinase-1; TGFβ-1, transforming growth factor β-1; MMP-7, matrix metalloproteinase-7; BLM, bleomycin sulfate.

tissue damage and fibrosis in a 14 day mouse bleomycin model.

*AM966 decreases mortality and fibrosis at late time points after bleomycin injury*

To assess the beneficial effects of $LPA_1$ receptor antagonism on survival, mice received an intratracheal instillation of 5 units·kg$^{-1}$ of bleomycin and were treated with AM966 (30 mg·kg$^{-1}$, BID) for a period of 21 days (Figure 9A). In response to bleomycin alone, 60% of the mice were dead by day 12 with majority of the mortalities occurring between days 7 and 9. In the AM966-treated group, only 2 out of 10 mice died and the first death did not occur until day 12, demonstrating an increase in both the magnitude and duration of the survival effect. In a separate, longer term study, AM966 decreased BALF collagen concentrations as late as day 28 after bleomycin (3.0 unit·kg$^{-1}$) injury (Figure 9B).

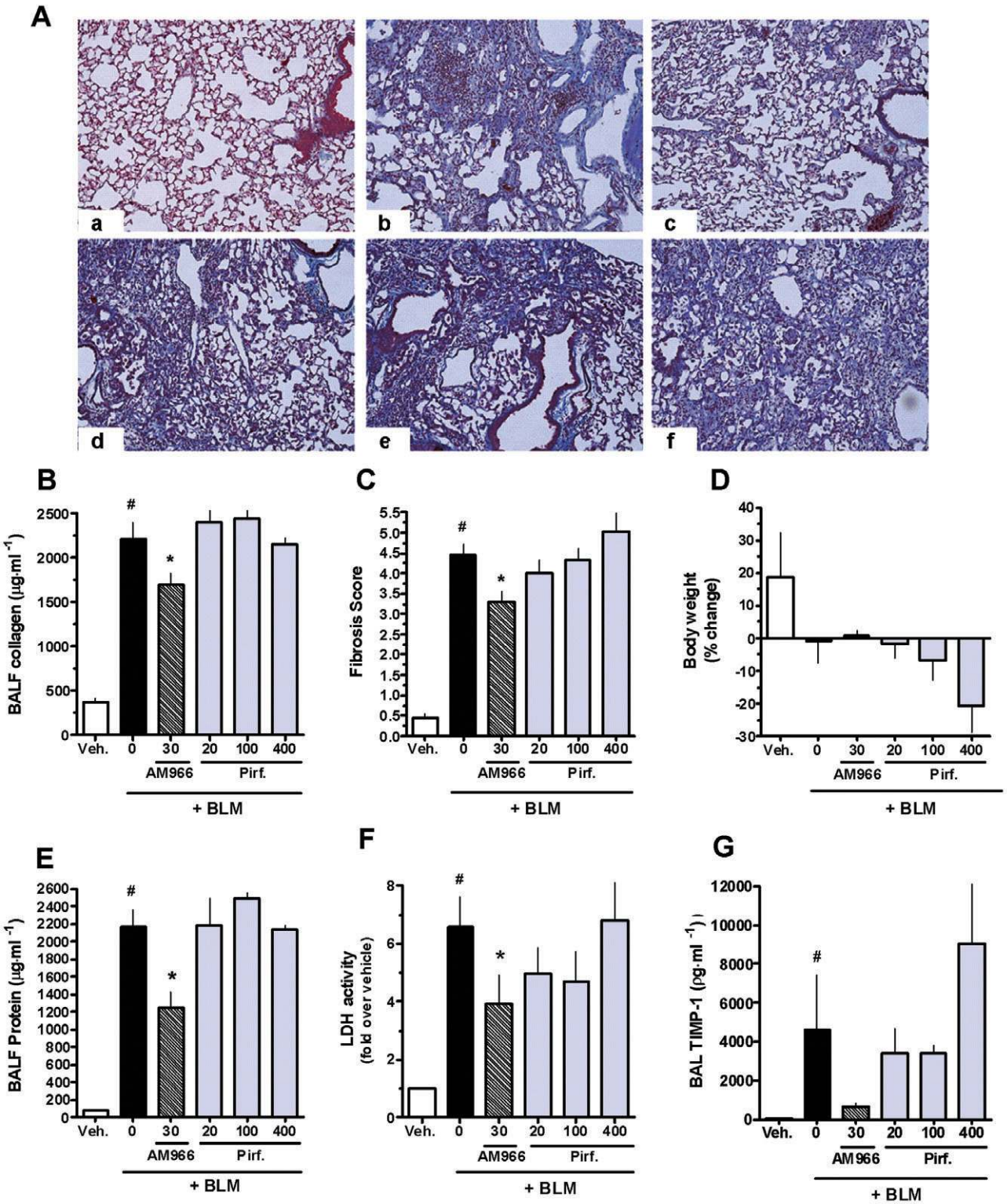


**Figure 8** AM966 demonstrates greater efficacy than pirfenidone after i.t. instillation of bleomycin. Mice were given intratracheal bleomycin sulfate (BLM; 3.0 units·kg$^{-1}$) or saline vehicle (Veh.) followed by oral administration of AM966 (30 mg·kg$^{-1}$, BID) or pirfenidone (20, 100 and 400 mg·kg$^{-1}$, BID) for a period of 14 days. Representative (A, panels a–f.) Trichrome-stained images (100× magnification) of lungs from mice treated with (a) vehicle, (b) BLM, (c) BLM + AM966 (30 mg·kg$^{-1}$, QD), (d) BLM + pirfenidone (20 mg·kg$^{-1}$, BID), (e) BLM + pirfenidone (100 mg·kg$^{-1}$, BID) and (f) BLM + pirfenidone (400 mg·kg$^{-1}$, BID). (B) soluble collagen concentrations in BALF (C) Histopathological scoring of lung fibrosis (D) Percentage change in mouse body weight (E) total protein in BALF (F) LDH activity and (G) TIMP-1 concentration are also shown. Data represent the mean ± standard error of the mean of $n = 4$–6 mice per group. # denotes a significant increase ($P < 0.05$) compared to vehicle control. * denotes a significant decrease ($P < 0.05$) compared to BLM. QD, once a day; BID, twice a day; BALF, bronchoalveolar lavage fluid; LDH, lactate dehydrogenase; TIMP-1, tissue inhibitor of metalloproteinase-1.

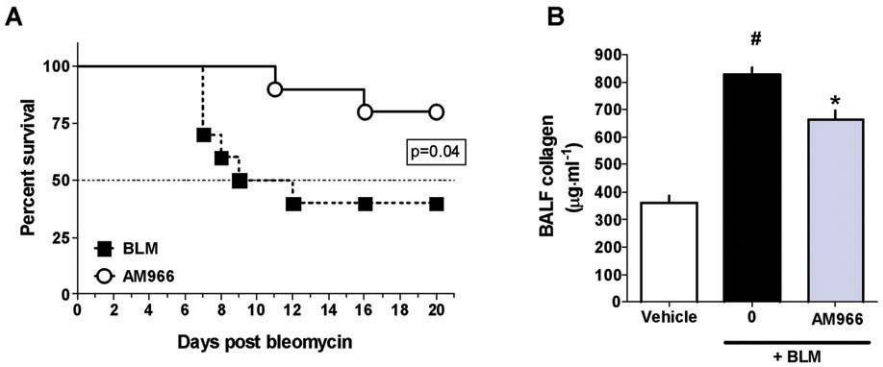


**Figure 9** Effects of AM966 on mouse survival and lung fibrosis 21–28 days after BLM administration. (A) AM966 (30 mg·kg$^{-1}$) significantly ($P = 0.04$) increased mouse survival over a 21 day period following i.t. instillation of BLM (5.0 units·kg$^{-1}$). (B) AM966 (30 mg·kg$^{-1}$) significantly ($P < 0.05$) decreased BALF collagen 28 days after i.t. instillation of BLM (3.0 units·kg$^{-1}$). # denotes a significant increase ($P < 0.05$) compared to vehicle control. * denotes a significant decrease ($P < 0.05$) compared to BLM. BLM, bleomycin sulfate; BALF, bronchoalveolar lavage fluid.

## Discussion

IPF is a devastating and grievous condition for which the only beneficial treatment modality is lung transplantation. Although a number of potential therapeutic targets are being investigated, no approved course of treatment currently exists that halts the progression of IPF and prolongs survival (Scotton and Chambers, 2007). As a result, there is a large unmet medical need for the identification of novel therapeutic strategies for treating IPF. Recently, some compelling findings by Tager *et al*. (2008) shed new light on this therapeutic area and identified LPA as a novel lysophospholipid mediator of pulmonary vascular leakage and fibroblast migration associated with IPF. Specifically, analysis of LPA receptor expression levels in IPF patients and preclinical studies using a mouse $LPA_1$ receptor knockout mouse identified the signalling through $LPA_1$ receptors as a potential pathogenic pathway in IPF. In addition to the fibrogenic role of $LPA_1$ receptors in the lung, Pradere *et al*. (2007) demonstrated a pathological role for these receptors in renal fibrosis. Using a UUO model, this group showed a reduction in tubulointerstitial fibrosis in $LPA_1$ knockout mice. In addition, administration of an $LPA_{1,3}$ selective antagonist (Ki16425) reduced kidney fibrosis and the expression of TGFβ and CTGF after UUO in wild-type mice. Thus, these and other studies have highlighted the role of LPA signalling in fibrotic disease and have identified the $LPA_1$ receptor as a therapeutic target for treating lung and kidney fibrosis. For this reason, we developed a novel $LPA_1$ receptor selective antagonist (AM966) and used the mouse bleomycin model to evaluate the potential of AM966 as a treatment for IPF.

Prior to initiating AM966 efficacy studies, we analysed the time- and dose-dependent effects of bleomycin on several BALF biomarkers that have been correlated with the severity of IPF or are known to be regulated by or exhibit crosstalk with LPA. LDH is an indicator of tissue damage and TIMP-1, TGFβ1, hyaluronan and MMP-7 are mediators of lung inflammation and fibrosis. These biomarkers are increased in both animal models of lung injury and in association with human lung fibrosis (Bjermer *et al*., 1989; Broekelmann *et al*., 1991; Drent *et al*., 1996; Swiderski *et al*., 1998; Rosas *et al*., 2008; Ou *et al*., 2009). Thus, by characterizing the time-dependent effects of bleomycin on these various markers we provided a framework for our interpretation of the mechanism(s) by which AM966 reduces lung inflammation and fibrosis. Based on the BALF and tissue-specific endpoints, AM966 appears to not only reduce the lung tissue damage, vascular leakage and inflammation that occur in the acute (3–7 day) phase after bleomycin injury, but it also decreases cytokine production and attenuates tissue remodelling and fibrosis in the chronic (14–28 day) phase.

It must be noted that, although AM966 is 100-fold more selective for human $LPA_1$ receptor over the other LPA receptors based on calcium flux data, the selectivity for mouse $LPA_1$ receptor is only 10-fold greater than that for mouse $LPA_3$ receptors. Because the plasma concentrations are above the $IC_{50}$ for mouse $LPA_3$ receptors during the first 8 h following a dose of 10 mg·kg$^{-1}$ (see Figure 3 and Table 1), it is likely that some of the effects observed in this report are mediated by $LPA_3$ receptors. This is particularly true at the high (30 and 60 mg·kg$^{-1}$) AM966 doses, for which peak plasma concentrations are predicted to be above the $IC_{50}$ for mouse $LPA_1$ and $LPA_3$ receptors for at least the first 8 h after dosing. Although the anti-fibrotic effects of AM966 are consistent with the findings of Tager *et al*. using the $LPA_1$ knockout mice, AM966 treatment produced a much greater reduction in inflammatory cells all time points tested. Interestingly, $LPA_{1-3}$ receptors have all been implicated in the regulation of lung inflammation (Saatian *et al*., 2006). Therefore, the anti-inflammatory effects of AM966 seen in these studies, both in terms of cellular infiltration and cytokine production in the lung, may be mediated in part via a reduction in $LPA_3$ signalling. Recent studies have also shown that $LPA_2$ receptors are mediators of lung fibrosis in both mice and humans (Xu *et al*., 2009) and regulate myofibroblast transformation and TGFβ production by human mesenchymal stem cells in culture (Jeon *et al*., 2008). The work by Xu *et al*. expanded upon the work of Tager *et al*. and suggested that $LPA_2$ receptors may regulate TGFβ activation and matrix synthesis, whereas $LPA_1$ receptors promote inflammation and vascular leakage associated with IPF. However, because the $IC_{50}$ for mouse $LPA_2$ receptors for AM966 is approximately 25 μM (Table 1), the effects described in our studies are unlikely to result from $LPA_2$ receptor antago-

nism. In terms of treating human disease, AM966 is at least 100-fold more selective for human $LPA_1$ receptors relative to any of the other LPA receptors. Furthermore, to address the issue of receptor selectivity, we are currently developing LPA receptor antagonists with greater selectivity for mouse $LPA_1$ receptors.

Of the LPA receptor antagonists that have been developed thus far, the $LPA_{1,3}$ antagonist Ki16425 has shown some therapeutic potential. Ki16426 has been used in a number of *in vitro* and *in vivo* studies (Ohta *et al*., 2003; Boucharaba *et al*., 2006) and has been shown to reduce renal fibrosis in a mouse UUO model (Pradere *et al*., 2007). Although the *in vitro* pharmacokinetic profiles of Ki16425 and AM966 are similar, the *in vivo* pharmacokinetic characteristics of AM966 are better in that AM966 is orally bioavailable, whereas Ki16425 is not and requires a subcutaneous route of administration.

Mechanistically, AM966 appears to exert its beneficial effects via multiple modes of action. Tissue injury initiates a precise series of molecular and cellular events, including (i) homeostasis; (ii) inflammation; (iii) cellular proliferation, migration and differentiation; (iv) matrix and tissue remodelling; and finally, (v) wound contracture and scar formation. It is widely recognized that many of these events are controlled by the coordinated release of biochemical factors within and around the site of injury (Wynn, 2008). In terms of $LPA_1$ receptors, it is believed that, following initial tissue injury, LPA is released into the lung interstitium via plasma exudation from the surrounding vascular compartment (Ley and Zarbock, 2008). These increased local LPA concentrations then act on $LPA_1$ receptors to promote vascular leakage, potentiate epithelial damage and recruit fibroblasts to the region of injury. As shown by our 3 day bleomycin model data, AM966 decreased protein content and LDH activity in the lung, indicating a potential for AM966 to reduce the LPA-mediated effects on vascular leakage and epithelial cell death that occur in IPF and other interstitial lung diseases. As the initial injury progresses, it is hypothesized that pathologically elevated concentrations of LPA may continue to activate $LPA_1$ receptors on pulmonary cells, thereby potentiating tissue inflammation and stimulating excessive ECM production. By day 7, when both inflammatory cell infiltration and fibrosis are observed in the bleomycin model (Cuzzocrea *et al*., 2007), AM966 reduced both of these parameters, indicating a continued ability of AM966 to antagonize $LPA_1$-mediated inflammation and scar tissue production. By day 14, when inflammation is resolving and fibrosis is at its peak, AM966 continues to decrease collagen production as well as inflammation. In addition, AM966 reduces BALF concentrations of TGFβ as well as other cytokines and proteases that are associated with the progression of lung fibrosis (Oga *et al*., 2009). Although bleomycin injury-induced fibrosis in mice is different from that observed in IPF, the findings of Tager *et al*. (2008) suggest that $LPA_1$ receptors are involved in both scenarios. Furthermore, these findings continue to support a very complex inflammatory and fibrotic role for $LPA_1$ receptors after lung injury and demonstrate that antagonism of $LPA_1$ receptors is sufficient to modify these pathological endpoints. Finally at days 21–28, although fibrosis is beginning to resolve, a significant reduction in collagen by AM966 was still observed. Furthermore, the combined effects of AM966 throughout this entire wound healing process, from initial injury to wound resolution, manifested itself in increased survival of AM966-treated mice compared to bleomycin controls, over the 21 survival day study.

The histopathological findings in IPF patients are highly varied and retrospective analyses of necropsy samples from IPF patients have revealed clinical features such as diffuse alveolar damage, usual interstitial pneumonia, metaplastic squamous epithelium and inflammatory cell infiltration (Tiitto *et al*., 2006). Via its pleiotropic effects on tissue damage, inflammation, vascular leakage and fibrosis, LPA may regulate numerous aspects of IPF pathogenesis through $LPA_1$ receptors. As a result, we believe that AM966 may target multiple aspects of the disease, thereby conferring greater therapeutic efficacy in comparison to approaches targeted on a single mechanism. Plasma exudation into the alveolar space and pulmonary interstitium is believed to be a major source of LPA in the IPF lung. Thus, the AM966-mediated reduction in vascular leakage may diminish the plasma-derived increases in LPA, which help to potentiate IPF disease progression. The ability of AM966 to reduce numerous BALF cytokines provides further mechanistic insight into the pathological role of $LPA_1$ receptors in lung inflammation and fibrosis. In addition, it may aid in identifying BALF biomarkers that can be used to extrapolate AM966 pre-clinical efficacy to the clinical setting.

One of the most interesting findings of this report was our comparison of AM966 and pirfenidone in the 14 day bleomycin model. Pirfenidone is a broad spectrum anti-fibrotic agent that is currently approved in Japan for the treatment of IPF and is in Phase III clinical trials in the United States for the same indication. Despite the limited data regarding its mode of action, pirfenidone has demonstrated anti-fibrotic effects in cell culture and in a number of pre-clinical lung, liver and kidney fibrosis models (Kakugawa *et al*., 2004; Oku *et al*., 2008; Lin *et al*., 2009; RamachandraRao *et al*., 2009; Zhao *et al*., 2009). The anti-fibrotic effects of pirfenidone are attributed to its ability to regulate TGFβ signalling, as well as that of other cytokines, and to scavenge free radicals (Misra and Rabideau, 2000; Oku *et al*., 2008). Using doses within the published range for pirfenidone in our mouse bleomycin studies, we conducted a direct head-to-head comparison between AM966 and pirfenidone. AM966 demonstrated greater efficacy than pirfenidone at all endpoints tested, whereas pirfenidone showed no therapeutic activity compared to bleomycin alone. This finding was unexpected based on the efficacy of pirfenidone in previously published mouse bleomycin studies (Kakugawa *et al*., 2004; Oku *et al*., 2008). In contrast to the data in Figure 6D that demonstrate a maintenance of mouse body weight at the 30 and 60 $mg \cdot kg^{-1}$ doses, AM966 did not maintain body weight in the studies involving pirfenidone (Figure 8E). This lack of a body weight effect was most likely due to the increased dose of bleomycin (3.0 $units \cdot kg^{-1}$ vs. 1.5 $units \cdot kg^{-1}$) that was employed in the pirfenidone studies (Figure 8E), relative to those described in Figure 6D. It must also be noted that in previous studies where pirfenidone was shown to reduce lung fibrosis, bleomycin was administered via i.v. injection over a 5 day period at the beginning of the study (Kakugawa *et al*., 2004; Oku *et al*., 2008). This systemic route of administration is sufficient when trying to mimic a chemotherapeutic dosing regime, but

requires a long period of time (6–8 weeks) for the development of lung fibrosis (Walters and Kleeberger, 2008). In contrast, our studies employed a single intratracheal instillation of bleomycin on the first day of the study. Intratracheal instillation of bleomycin elicits a peak fibrotic response within 2–3 weeks and produces a more variable distribution of fibrotic foci. Thus, the discrepancy in pirfenidone efficacy between our study and those of other investigators may be due to differences in the route of bleomycin administration and the resulting progression of lung injury and fibrosis.

In conclusion, our findings confirm a role for LPA$_1$ receptors in inflammation, production of extracellular matrix and tissue remodelling following lung injury. In addition, we demonstrate that antagonizing LPA$_1$ receptors in the lung with a small molecule has effects consistent with those observed in the LPA$_1$ receptor knockout mouse. Therefore, the ability of AM966 to modify these pathological endpoints further supports LPA$_1$ receptors as a novel clinical target in treating IPF and paves the way for the clinical development of an oral, 'first in class' LPA$_1$ receptor antagonist to treat IPF and other lung diseases characterized by pathological inflammation, oedema and fibrosis.

## Conflict of interest

All authors of this manuscript are paid employees of Amira Pharmaceuticals.

## References

Alexander SPH, Mathie A, Peters JA (2009). Guide to Receptors and Channels (GRAC), 4th edn. *Br J Pharmacol* **158** (Suppl. 1): S1–S254.

Andersson-Sjoland A, de Alba CG, Nihlberg K, Becerril C, Ramirez R, Pardo A *et al*. (2008). Fibrocytes are a potential source of lung fibroblasts in idiopathic pulmonary fibrosis. *Int J Biochem Cell Biol* **40**: 2129–2140.

Anliker B, Chun J (2004). Cell surface receptors in lysophospholipid signaling. *Semin Cell Dev Biol* **15**: 457–465.

Ashcroft T, Simpson JM, Timbrell V (1988). Simple method of estimating severity of pulmonary fibrosis on a numerical scale. *J Clin Pathol* **41**: 467–470.

Bjermer L, Lundgren R, Hallgren R (1989). Hyaluronan and type III procollagen peptide concentrations in bronchoalveolar lavage fluid in idiopathic pulmonary fibrosis. *Thorax* **44**: 126–131.

Boucharaba A, Serre CM, Guglielmi J, Bordet JC, Clezardin P, Peyruchaud O (2006). The type 1 lysophosphatidic acid receptor is a target for therapy in bone metastases. *Proc Natl Acad Sci U S A* **103**: 9643–9648.

Broekelmann TJ, Limper AH, Colby TV, McDonald JA (1991). Transforming growth factor beta 1 is present at sites of extracellular matrix gene expression in human pulmonary fibrosis. *Proc Natl Acad Sci U S A* **88**: 6642–6646.

Cuzzocrea S, Genovese T, Failla M, Vecchio G, Fruciano M, Mazzon E *et al*. (2007). Protective effect of orally administered carnosine on bleomycin-induced lung injury. *Am J Physiol Lung Cell Mol Physiol* **292**: L1095–L1104.

Drent M, Cobben NA, Henderson RF, Wouters EF, van Dieijen-Visser M (1996). Usefulness of lactate dehydrogenase and its isoenzymes as indicators of lung damage or inflammation. *Eur Respir J* **9**: 1736–1742.

Gabbiani G, Ryan GB, Majne G (1971). Presence of modified fibroblasts in granulation tissue and their possible role in wound contraction. *Experientia* **27**: 549–550.

Izbicki G, Segel MJ, Christensen TG, Conner MW, Breuer R (2002). Time course of bleomycin-induced lung fibrosis. *Int J Exp Pathol* **83**: 111–119.

Jankov RP, Luo X, Demin P, Aslam R, Hannam V, Tanswell AK *et al*. (2002). Hepoxilin analogs inhibit bleomycin-induced pulmonary fibrosis in the mouse. *J Pharmacol Exp Ther* **301**: 435–440.

Jeon ES, Moon HJ, Lee MJ, Song HY, Kim YM, Cho M *et al*. (2008). Cancer-derived lysophosphatidic acid stimulates differentiation of human mesenchymal stem cells to myofibroblast-like cells. *Stem Cells* **26**: 789–797.

Kakugawa T, Mukae H, Hayashi T, Ishii H, Abe K, Fujii T *et al*. (2004). Pirfenidone attenuates expression of HSP47 in murine bleomycin-induced pulmonary fibrosis. *Eur Respir J* **24**: 57–65.

Ley K, Zarbock A (2008). From lung injury to fibrosis. *Nat Med* **14**: 20–21.

Lin X, Yu M, Wu K, Yuan H, Zhong H (2009). Effects of pirfenidone on proliferation, migration, and collagen contraction of human Tenon's fibroblasts in vitro. *Invest Ophthalmol Vis Sci* **50**: 3763–3770.

Misra HP, Rabideau C (2000). Pirfenidone inhibits NADPH-dependent microsomal lipid peroxidation and scavenges hydroxyl radicals. *Mol Cell Biochem* **204**: 119–126.

Oga T, Matsuoka T, Yao C, Nonomura K, Kitaoka S, Sakata D *et al*. (2009). Prostaglandin F(2alpha) receptor signaling facilitates bleomycin-induced pulmonary fibrosis independently of transforming growth factor-beta. *Nat Med* **15**: 1426–1430.

Ohta H, Sato K, Murata N, Damirin A, Malchinkhuu E, Kon J *et al*. (2003). Ki16425, a subtype-selective antagonist for EDG-family lysophosphatidic acid receptors. *Mol Pharmacol* **64**: 994–1005.

Oku H, Shimizu T, Kawabata T, Nagira M, Hikita I, Ueyama A *et al*. (2008). Antifibrotic action of pirfenidone and prednisolone: different effects on pulmonary cytokines and growth factors in bleomycin-induced murine pulmonary fibrosis. *Eur J Pharmacol* **590**: 400–408.

Ou XM, Li WC, Liu DS, Li YP, Wen FQ, Feng YL *et al*. (2009). VEGFR-2 antagonist SU5416 attenuates bleomycin-induced pulmonary fibrosis in mice. *Int Immunopharmacol* **9**: 70–79.

Pradere JP, Klein J, Gres S, Guigne C, Neau E, Valet P *et al*. (2007). LPA1 Receptor Activation Promotes Renal Interstitial Fibrosis. *J Am Soc Nephrol*.

Raghu G, Weycker D, Edelsberg J, Bradford WZ, Oster G (2006). Incidence and prevalence of idiopathic pulmonary fibrosis. *Am J Respir Crit Care Med* **174**: 810–816.

RamachandraRao SP, Zhu Y, Ravasi T, McGowan TA, Toh I, Dunn SR *et al*. (2009). Pirfenidone is renoprotective in diabetic kidney disease. *J Am Soc Nephrol* **20**: 1765–1775.

Rosas IO, Richards TJ, Konishi K, Zhang Y, Gibson K, Lokshin AE *et al*. (2008). MMP1 and MMP7 as potential peripheral blood biomarkers in idiopathic pulmonary fibrosis. *PLoS Med* **5**: e93.

Saatian B, Zhao Y, He D, Georas SN, Watkins T, Spannhake EW *et al*. (2006). Transcriptional regulation of lysophosphatidic acid-induced interleukin-8 expression and secretion by p38 MAPK and JNK in human bronchial epithelial cells. *Biochem J* **393**: 657–668.

Scotton CJ, Chambers RC (2007). Molecular targets in pulmonary fibrosis: the myofibroblast in focus. *Chest* **132**: 1311–1321.

Selman M, Pardo A (2002). Idiopathic pulmonary fibrosis: an epithelial/fibroblastic cross-talk disorder. *Respir Res* **3**: 3.

Swaney JS, Roth DM, Olson ER, Naugle JE, Meszaros JG, Insel PA (2005). Inhibition of cardiac myofibroblast formation and collagen synthesis by activation and overexpression of adenylyl cyclase. *Proc Natl Acad Sci U S A* **102**: 437–442.

Swiderski RE, Dencoff JE, Floerchinger CS, Shapiro SD, Hunninghake GW (1998). Differential expression of extracellular matrix remodeling genes in a murine model of bleomycin-induced pulmonary fibrosis. *Am J Pathol* **152**: 821–828.

Tager AM, LaCamera P, Shea BS, Campanella GS, Selman M, Zhao Z *et al*. (2008). The lysophosphatidic acid receptor LPA1 links pulmonary fibrosis to lung injury by mediating fibroblast recruitment and vascular leak. *Nat Med* **14**: 45–54.

Tanjore H, Xu XC, Polosukhin VV, Degryse AL, Li B, Han W *et al*. (2009). Contribution of epithelial-derived fibroblasts to bleomycin-induced lung fibrosis. *Am J Respir Crit Care Med* **180**: 657–665.

Tiitto L, Bloigu R, Heiskanen U, Paakko P, Kinnula VL, Kaarteenaho-Wiik R (2006). Relationship between histopathological features and the course of idiopathic pulmonary fibrosis/usual interstitial pneumonia. *Thorax* **61**: 1091–1095.

Tomasek JJ, Gabbiani G, Hinz B, Chaponnier C, Brown RA (2002). Myofibroblasts and mechano-regulation of connective tissue remodelling. *Nat Rev Mol Cell Biol* **3**: 349–363.

Walters DM, Kleeberger SR (2008). Mouse models of bleomycin-induced pulmonary fibrosis. In: Enna SJ (ed.). *Current Protocols in Pharmacology*. John Wiley & Sons: New York, pp. 5.46.1–5.46.17.

Watterson KR, Lanning DA, Diegelmann RF, Spiegel S (2007). Regulation of fibroblast functions by lysophospholipid mediators: potential roles in wound healing. *Wound Repair Regen* **15**: 607–616.

Willis BC, Liebler JM, Luby-Phelps K, Nicholson AG, Crandall ED, du Bois RM *et al*. (2005). Induction of epithelial-mesenchymal transition in alveolar epithelial cells by transforming growth factor-beta1: potential role in idiopathic pulmonary fibrosis. *Am J Pathol* **166**: 1321–1332.

Wilson MS, Wynn TA (2009). Pulmonary fibrosis: pathogenesis, etiology and regulation. *Mucosal Immunol* **2**: 103–121.

Wynn TA (2008). Cellular and molecular mechanisms of fibrosis. *J Pathol* **214**: 199–210.

Xu MY, Porte J, Knox AJ, Weinreb PH, Maher TM, Violette SM *et al*. (2009). Lysophosphatidic acid induces alphavbeta6 integrin-mediated TGF-beta activation via the LPA2 receptor and the small G protein G alpha(q). *Am J Pathol* **174**: 1264–1279.

Zhao XY, Zeng X, Li XM, Wang TL, Wang BE (2009). Pirfenidone Effectively Inhibits Carbon Tetrachloride- and Albumin Complex-Induced Liver Fibrosis in Rodents by Preventing Activation of Hepatic Stellate Cells. *Clin Exp Pharmacol Physiol* **36**: 963–968. Epub 27 April 2009